

UNCLASSIFIED

AD 418711

DEFENSE DOCUMENTATION CENTER

FOR

SCIENTIFIC AND TECHNICAL INFORMATION

CAMERON STATION, ALEXANDRIA, VIRGINIA



UNCLASSIFIED

NOTICE: When government or other drawings, specifications or other data are used for any purpose other than in connection with a definitely related government procurement operation, the U. S. Government thereby incurs no responsibility, nor any obligation whatsoever; and the fact that the Government may have formulated, furnished, or in any way supplied the said drawings, specifications, or other data is not to be regarded by implication or otherwise as in any manner licensing the holder or any other person or corporation, or conveying any rights or permission to manufacture, use or sell any patented invention that may in any way be related thereto.

AEDC-TDR-63-192

CLASSIFIED BY CDC
AS AD 10418011



**BOUNDARY-LAYER CHARACTERISTICS
AT MACH NUMBERS 2 THROUGH 5
IN THE TEST SECTION OF THE 12-INCH
SUPERSONIC TUNNEL (D)**

By

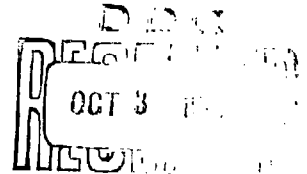
64-17

**D. R. Bell
von Kármán Gas Dynamics Facility
ARO, Inc.**

TECHNICAL DOCUMENTARY REPORT NO. AEDC-TDR-63-192

September 1963

AFSC Program Area 040A



(Prepared under Contract No. AF 40(600)-1000 by ARO, Inc., contract operator of AEDC, Arnold Air Force Station, Tenn.)

418711

**ARNOLD ENGINEERING DEVELOPMENT CENTER
AIR FORCE SYSTEMS COMMAND
UNITED STATES AIR FORCE**

NOTICES

Qualified requesters may obtain copies of this report from DDC, Cameron Station, Alexandria, Va. Orders will be expedited if placed through the librarian or other staff member designated to request and receive documents from DDC.

When Government drawings, specifications or other data are used for any purpose other than in connection with a definitely related Government project, the United States Government thereby incurs no responsibility whatsoever; and the fact that the Government may have developed, furnished, or in any way supplied the said drawings, specifications, or other data, is not to be regarded by implication or otherwise as in any manner licensing the holder or any other person or corporation, or conveying any rights or permission to manufacture, use, or sell any patented invention that may in any way be related thereto.

BOUNDARY-LAYER CHARACTERISTICS
AT MACH NUMBERS 2 THROUGH 5
IN THE TEST SECTION OF THE 12-INCH
SUPERSONIC TUNNEL (D)

By
D. R. Bell
von Kármán Gas Dynamics Facility
ARO, Inc.
a subsidiary of Sverdrup and Parcel, Inc.

September 1963
ARO Project No. VD2257


ABSTRACT


As part of a general tunnel calibration program, an investigation was made of the boundary-layer characteristics at Mach numbers 2, 3, 4, and 5 in the test section of the 12-Inch Supersonic Tunnel (D). The boundary-layer measurements were made at one longitudinal station (near the pitch sector center of rotation) on the centerline of both the flexible plate and sidewall. Measurements were also made at vertical locations on the sidewall between the sidewall centerline and the upper

The boundary-layer total thickness, displacement thickness, and momentum thickness are presented at each Mach number over a Reynolds number range corresponding, in general, to tunnel stagnation pressures between 5 and 60 psia. At each Mach number, the variation of displacement thickness on the sidewall between the centerline and the upper flexible plate is presented as is a correlation of the flexible plate displacement thickness with experimental data obtained in other wind tunnels. Velocity profiles and test section Mach numbers are presented to indicate variations with Reynolds number.

PUBLICATION REVIEW

This report has been reviewed and publication is approved.


Darreld K. Calkins
Major, USAF
AF Representative, VKF
DCS/Test


Jean A. Jack
Colonel, USAF
DCS/Test

CONTENTS

	<u>Page</u>
ABSTRACT	ii
NOMENCLATURE	iv
1.0 INTRODUCTION	1
2.0 APPARATUS	
2.1 Wind Tunnel	1
2.2 Instrumentation	1
3.0 PROCEDURE	2
4.0 RESULTS AND DISCUSSION	2
5.0 SUMMARY	5
REFERENCES	5

ILLUSTRATIONS

Figure

1. The 12-Inch Supersonic Tunnel (D)	8
2. Boundary-Layer Rake Locations	9
3. Boundary-Layer Thickness Ratios, $g = \delta^*/\delta$ and $H = \delta^*/\theta$, on the Flexible Plate and Sidewall Centerlines at Mach Numbers 2 through 5	10
4. Velocity Profiles on the Flexible Plate and Sidewall Centerlines at Mach Numbers 4 and 5	11
5. Total, Displacement, and Momentum Thickness on the Flexible Plate and Sidewall Centerlines at Mach Numbers 2 through 5	12
6. Mach Number and Displacement Thickness Variation with Reynolds Number at Mach Numbers 4 and 5	13
7. Comparison between Experimental and Theoretical Values of Total and Displacement Thickness on the Flexible Plate and Sidewall Centerline at Mach Numbers 2 through 5	14
8. Variation of the Sidewall Displacement Thickness between the Centerline and Upper Flexible Plate at Mach Numbers 2 through 5	15
9. Flexible Plate Displacement Thickness Correlation at Mach Numbers 1.5 through 5	16

NOMENCLATURE

a_0	Speed of sound at stagnation conditions, ft/sec
g	Ratio of boundary-layer displacement thickness to total thickness, δ^*/δ
H	Ratio of boundary-layer displacement thickness to momentum thickness, δ^*/θ
K	$0.0131 \left(\frac{\mu_0}{\rho_0 a_0} \right)^{1/2}$
M_∞	Free-stream Mach number
M^*	Displacement thickness parameter, $U/\rho_\infty U_\infty^2$
P_0	Stagnation pressure, psia
Re	Test section unit Reynolds number
U_y	Local velocity within the boundary layer at distance y from wall, ft/sec
U_∞	Free-stream velocity, ft/sec
X_E	Longitudinal distance of the nozzle aerodynamic exit plane referenced to nozzle throat location, in.
y	Distance normal to wall, in.
δ	Boundary-layer total thickness, in.
δ_L	Laminar sublayer thickness of the boundary layer, in.
δ^*	Boundary-layer displacement thickness, $\int_0^\delta \left(1 - \frac{\rho_y U_y}{\rho_\infty U_\infty} \right) dy$, in.
$\bar{\delta}^*$	Displacement thickness parameter, $\frac{\delta^*}{K X_E^{1/2}}$
θ	Boundary-layer total thickness, $\int_0^\delta \frac{\rho_y U_y}{\rho_\infty U_\infty} \left(1 - \frac{U_y}{U_\infty} \right) dy$, in.
μ_0	Coefficient of viscosity at stagnation conditions, lb sec/ft ²
ρ_0	Density at stagnation conditions, lb sec ² /ft ⁴
ρ_y	Local density within the boundary layer at distance y from wall, lb sec ² /ft ⁴
ρ_∞	Free-stream density, lb sec ² /ft ⁴

1.0 INTRODUCTION

A test program was conducted to calibrate, at the lower Reynolds numbers, the test section of the 12-Inch Supersonic Tunnel (D) of the von Kármán Gas Dynamics Facility (VKF), Arnold Engineering Development Center (AEDC), Air Force Systems Command (AFSC). As part of this calibration program the boundary-layer characteristics on the flexible plate and sidewall of the tunnel test section were obtained over the Reynolds number range from 0.02 to 0.69×10^6 per inch at Mach numbers 2, 3, 4, and 5. This report presents the results of the boundary-layer investigation and correlates the flexible plate displacement thickness with measurements in the

2.0 APPARATUS

2.1 WIND TUNNEL

The 12-Inch Supersonic Tunnel (D) (Fig. 1) is an intermittent, variable density wind tunnel with a manually adjusted, flexible-plate-type nozzle. The tunnel operates at Mach numbers from 1.5 to 5 at stagnation pressures from about 5 to 60 psia and at stagnation temperatures up to about 90°F. A detailed description of the tunnel is given in Ref. 1.

2.2 INSTRUMENTATION

The pressure data from the boundary-layer rake was measured with a "trapped" reference system. This system used a 5- or 30-psid transducer (referenced to a vacuum) to measure a reference pressure obtained from the outermost rake probe. When the reference pressure reached a desired level, a valve was closed, sealing the reference from the probe pressure; hence, "trapped" reference. The pressure differential existing between the rake probes and the trapped reference was then measured with either a 1- or 15-psid transducer.

The boundary-layer parameters, δ , δ^* , and θ were determined by methods and equations given in Ref. 2. The data was reduced by the VKF ERA 1102 computer.

Manuscript received August 1963.

The estimated maximum uncertainties of the boundary-layer thickness values presented are: total thickness, 7 percent; displacement thickness, 3 percent; and momentum thickness, 3 percent.

3.0 PROCEDURE

Boundary-layer measurements were made at one longitudinal station (near the pitch sector center of rotation) on the centerline of both the flexible plate and sidewall and at one-inch increments on the sidewall between the sidewall centerline and the upper flexible plate. Figure 2 presents a perspective drawing of the tunnel test section showing the various locations of the boundary-layer rake.

Although tests were made at Mach numbers 2, 3, 4, and 5 over the Reynolds number range of the tunnel, primary emphasis was placed on Reynolds numbers corresponding to stagnation pressures between 5 and 30 psia. Table 1 lists the specific condition at which measurements were made.

4.0 RESULTS AND DISCUSSION

Figure 3 shows a comparison of the theoretical values of the turbulent boundary-layer parameters, $g = \delta^*/\delta$, and $H = \delta^*/\theta$ obtained from Ref. 3, with the experimental values measured on the sidewall and flexible plate centerlines. The number beside each data point represents the experimental value of the velocity profile parameter N . The sidewall data are not presented at Mach numbers 4 and 5 because the experimental values of N were below the minimum value of 5 presented in Ref. 3. These lower values of N are characteristic of a laminar boundary layer.

The experimental values agree with theory at all Mach numbers presented with the exception of some values of the shape parameter H on the flexible plate centerline at Mach numbers 4 and 5. Those points which do not agree with the theory ($N = 7.1, 8.3$, and 10 at Mach 5 and $N = 14$ at Mach 4) are associated with the thicker laminar sublayers shown in the velocity profiles of Fig. 4 where the flow is becoming transitional in nature. This figure presents the boundary-layer velocity profile at Mach 4 and 5 in terms of the dimensionless parameter y/δ . The flexible plate boundary layer is characterized by a turbulent $1/N$ -power profile in its outer portion but has, at the lower Reynolds numbers, a relatively thick laminar sublayer represented by the linear fairing in the region adjacent to the wall (Ref. 4). The

sidewall centerline boundary layer exhibits laminar characteristics to the extent that its power profile parameter N is less than 5 at Mach 4 and 5; however, as the Reynolds number is increased, the value of N also increases as expected.

The flexible plate velocity profiles at the extremes of the Reynolds number ranges investigated (see Fig. 5) have been omitted from Fig. 4 because in their turbulent portions they are practically congruent with the $N = 7$ profiles shown. The sidewall profiles at the intermediate Reynolds numbers have been omitted since they fall between the extremes shown.

Figure 5 presents the variation with Reynolds number of the boundary-layer total thickness δ , displacement thickness δ^* , and momentum thickness θ on the flexible plate and sidewall centerlines. The increase in boundary-layer thickness δ , δ^* , and θ on the flexible plate between Reynolds numbers of 70 and 100 thousand per inch at Mach 5 and 40 and 80 thousand per inch at Mach 4 is reflected in the variation of the test section Mach number with Reynolds number. Figure 6 shows the Mach number and flexible plate displacement thickness variations at Mach numbers 4 and 5. Changes of Mach number with Reynolds number are seen to be in a direction which would be produced by the variation of the boundary-layer thickness and in turn nozzle area ratio. Referring back to Fig. 4, it is also interesting to note that the turbulent outer portion of the flexible plate boundary layer is similar throughout the Reynolds number range with the exception of an increase in the velocity profile parameter, N , at the Reynolds number where the minimum displacement thickness was measured ($Re/in.$ of 0.07×10^6 at Mach 5 and 0.040×10^6 at Mach 4).

In Fig. 7 the experimental values of the boundary-layer total and displacement thickness are compared with the theoretical values computed by the method of Tucker (Ref. 3). This method determines the turbulent boundary-layer development along an insulated surface with a pressure gradient. The theoretical skin friction coefficient used in the computations was calculated using an arithmetic-mean between the wall and stream temperature values for the viscosity calculations. Also a turbulent velocity profile parameter of $N = 7$ was assumed.

The flexible plate data presented for the maximum Reynolds number ($p_0 = 60$ psia) at Mach 2 and the minimum Reynolds number ($p_0 = 5$ psia) at Mach numbers 4 and 5 were obtained by a smooth curve extrapolation of the boundary-layer thickness variations with Reynolds number shown in Fig. 5.

Figure 8 shows the variation of the sidewall boundary-layer displacement thickness between the sidewall centerline and the upper flexible plate. The large decrease in displacement thickness as the top wall is approached at Mach 4 and 5, and to a lesser extent at Mach 3, is attributed to secondary cross-flows within the boundary layer. As discussed in Ref. 5, these cross-flows are the result of transverse static pressure gradients present in all non-axially symmetric nozzles.

Figure 9 presents a correlation of the displacement thickness measured on the flexible plate with experimental data measured in several other supersonic wind tunnels. This correlation is based upon a nondimensional displacement thickness parameter, $\bar{\delta}^*$.

where
$$\bar{\delta}^* = \frac{\delta^*}{K X_E^{1/2}}$$

and
$$K = 0.0131 \left(\frac{\mu_o}{\rho_o a_o} \right)^{1/2}$$

Reference 6 develops this relationship by rearranging the equations of Tucker (Ref. 3) to obtain a boundary-layer growth parameter independent of nozzle size and stagnation conditions.

In those instances where the position of the nozzle aerodynamic exit (location of last characteristic) is known, the experimentally determined values of δ^* are transferred to this point before computing $\bar{\delta}^*$. This transfer is accomplished by the method of Ref. 6. Where the position of the aerodynamic exit is unknown, $\bar{\delta}^*$ is computed directly from the measured value of δ^* and the distance from the throat to the point of measurement. Figure 9 indicates which method was used to compute the values of $\bar{\delta}^*$ shown.

Since Tucker's equations apply only to turbulent boundary-layer development, the tunnel D data which exhibited laminar sublayers are not included in Fig. 9. This figure shows that, for the most part, the tunnel D turbulent boundary-layer data correlates quite well with that of the other tunnels, although at Mach 4 and 5, values of $\bar{\delta}^*$ higher than the correlating values were obtained. At both of these Mach numbers, the high values of $\bar{\delta}^*$ occurred at the peak of a rapid increase in displacement thickness with Reynolds number ($Re/in. = 0.10 \times 10^6$ at Mach 5 and 0.330×10^6 at Mach 4, Fig. 5) while the values of $\bar{\delta}^*$ which correlated best were obtained at the maximum Reynolds numbers tested.

5.0 SUMMARY

The following results were obtained from an investigation of the test section boundary-layer conducted in the 12-Inch Supersonic Tunnel (D) of the von Kármán Gas Dynamics Facility:

1. With the exception of the sidewall centerline measurements at Mach 4 and 5, the test section boundary-layer characteristics were primarily turbulent.
2. The characteristics of the turbulent boundary layers agree well with theory except for the flexible plate boundary layers whose profiles exhibit well-defined laminar sublayers at Mach numbers 4 and 5. Here, the experimental values of H are higher than predicted by theory.
3. At Mach numbers 4 and 5, the variation of the test section Mach number with Reynolds number is associated with the variation of the flexible plate boundary-layer characteristics.
4. At Mach numbers 3, 4, and 5, the displacement thickness of the sidewall boundary layer decreases as the upper wall is approached. This decrease is attributed to secondary cross-flows within the boundary layer.
5. The flexible plate displacement thickness correlates with that of other supersonic wind tunnels when compared on the basis of the nondimensional parameter, δ^* .

REFERENCES

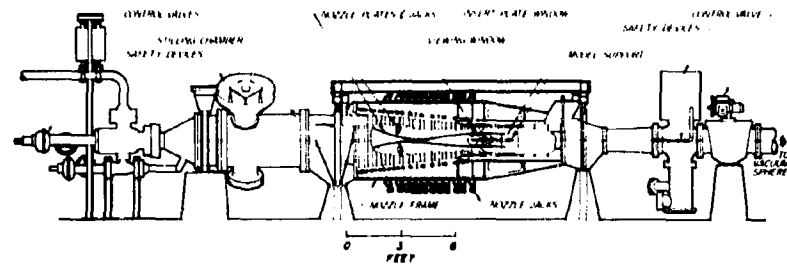
1. Test Facilities Handbook (5th Edition). "von Kármán Gas Dynamics Facility." Vol. 4, Arnold Engineering Development Center, July 1963.
2. Schlichting, Hermann. Boundary Layer Theory. McGraw-Hill, New York, 1955.
3. Tucker, M. "Approximate Calculation of Turbulent Boundary Layer Development in Compressible Flow." NACA-TN-2337, April 1951.
4. Donaldson, Coleman duP. "On the Form of the Turbulent Skin Friction Law and Its Extension to Compressible Flows." NACA-TN-2692, May 1952.

5. Brinich, Paul F. "Boundary Layer Measurements in 3.88- by 10-Inch Supersonic Channel." NACA-TN-2203, October 1950.
6. Maxwell, H., and Jacocks, J. L. "Nondimensional Calculation of Turbulent Boundary-Layer Development in Two-Dimensional Nozzles of Supersonic Wind Tunnels." AEDC-TN-61-153, January 1962.
7. Jones, Jerry. "An Investigation of the Boundary-Layer Characteristics in the Test Section of a 40 by 40-Inch Supersonic Tunnel." AEDC-TN-60-189, October 1960.
8. Jet Propulsion Laboratory Research Summary No. 36-6, Vol. II, January 1961.
9. Ying-Nien Yu. "A Summary of Design Techniques for Axisymmetric Hypersonic Wind Tunnels." AGARDograph 35, November 1958.
10. Goin, K. L. "Summary Calibration Report of the Ordnance Aerophysics Laboratory Supersonic Wind Tunnel." OAL Report 340-2, August 1957.
11. Thompson, M. J., and Wilson, R. E. "Aerodynamic Characteristics of Nozzles and Diffusers for Supersonic Wind Tunnels." DRL-281, Aeromechanics Section, Defense Research Laboratory, University of Texas, April 1951. AT1 103484.
12. Smith, K. G. and Winter, K. G. "Boundary Layer Growth in the Nozzles of the R. A. E. 8 ft x 8 ft Supersonic Wind Tunnel." RAE Technical Note No. AERO 2767, June 1961.
13. Ruptash, J. "Boundary Layer Measurements in the UTIA 5- by 7-Inch Supersonic Wind Tunnel." UTIA Report No. 16, May 1952.
14. Baron, Judson R. "Analytic Design of a Family of Supersonic Nozzles by the Friedrichs Method." WADC TR 54-279, June 1954.

TABLE 1
TEST CONDITIONS

M_∞	P_0 , psia	$Re/in. \times 10^{-6}$	Flexible Plate Centerline	Sidewall					
				ζ	Distance above ζ , in.				
					1	2	3	4	5
2	1	0.02	x	x	x	x	x	x	x
	5	0.11	x	x	x	x	x	x	x
	10	0.23	x	x	x	x	x	x	x
	15	0.33	x	x	x	x	x	x	x
	30	0.69	x	x	x	x	x	x	x
3	5	0.07	x	x	x	x	x	x	x
	10	0.14	x	x	x	x	x	x	x
	15	0.21	x	x	x	x	x	x	x
	20	0.28	x	x	x	x	x		
	30	0.39							x
	60	0.82	x	x	x	x	x	x	x
4	5	0.04	x	x	x	x	x		
	10	0.08	x	x	x	x	x		
	15	0.12	x	x	x	x	x		x
	20	0.16	x	x	x	x	x		x
	60	0.48	x	x	x	x	x		x
5	5	0.02	x						
	7	0.03	x	x		x	x	x	
	10	0.05	x	x	x	x	x	x	
	15	0.07	x	x	x	x	x	x	
	17	0.08	x	x	x	x	x	x	
	20	0.10	x	x	x		x	x	
	30	0.14		x	x		x	x	x
	40	0.19							x
60	0.29	x	x	x	x	x	x	x	

x Indicates where measurements were made



Assembly

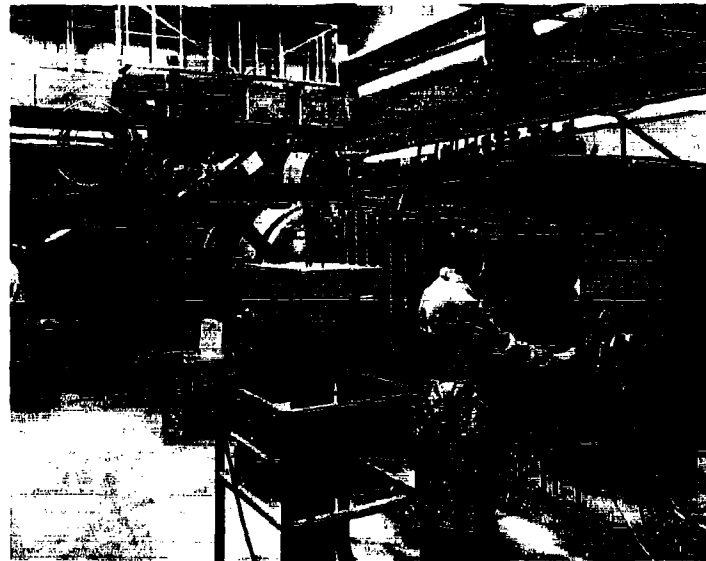


Fig. 1 The 12-inch Supersonic Tunnel (D)

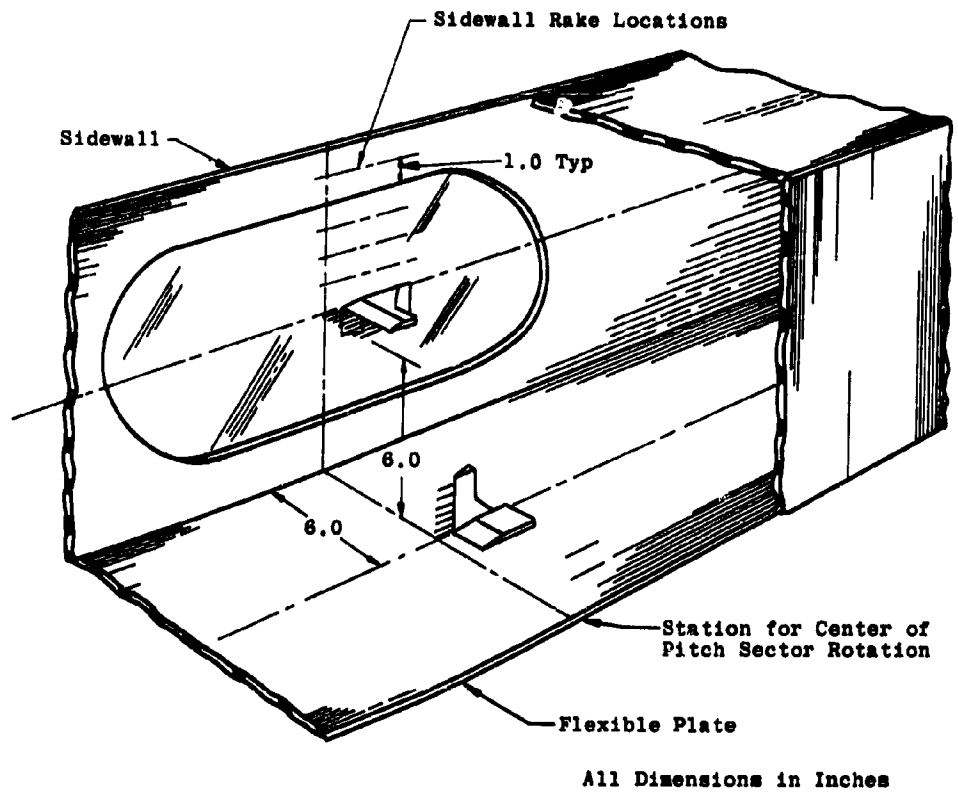


Fig. 2 Boundary-Layer Rake Locations

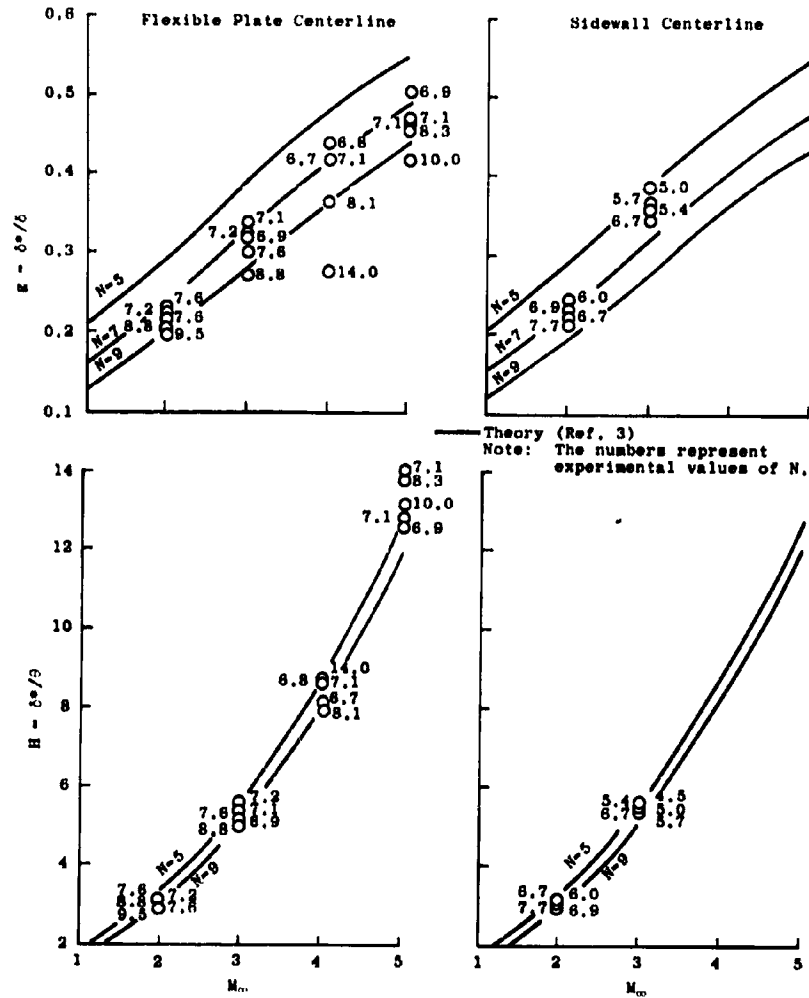


Fig. 3 Boundary-Layer Thickness Ratios, $g = \delta^*/\delta$ and $H = \delta^*/\theta$, on the Flexible Plate and Sidewall Centerlines at Mach Numbers 2 through 5

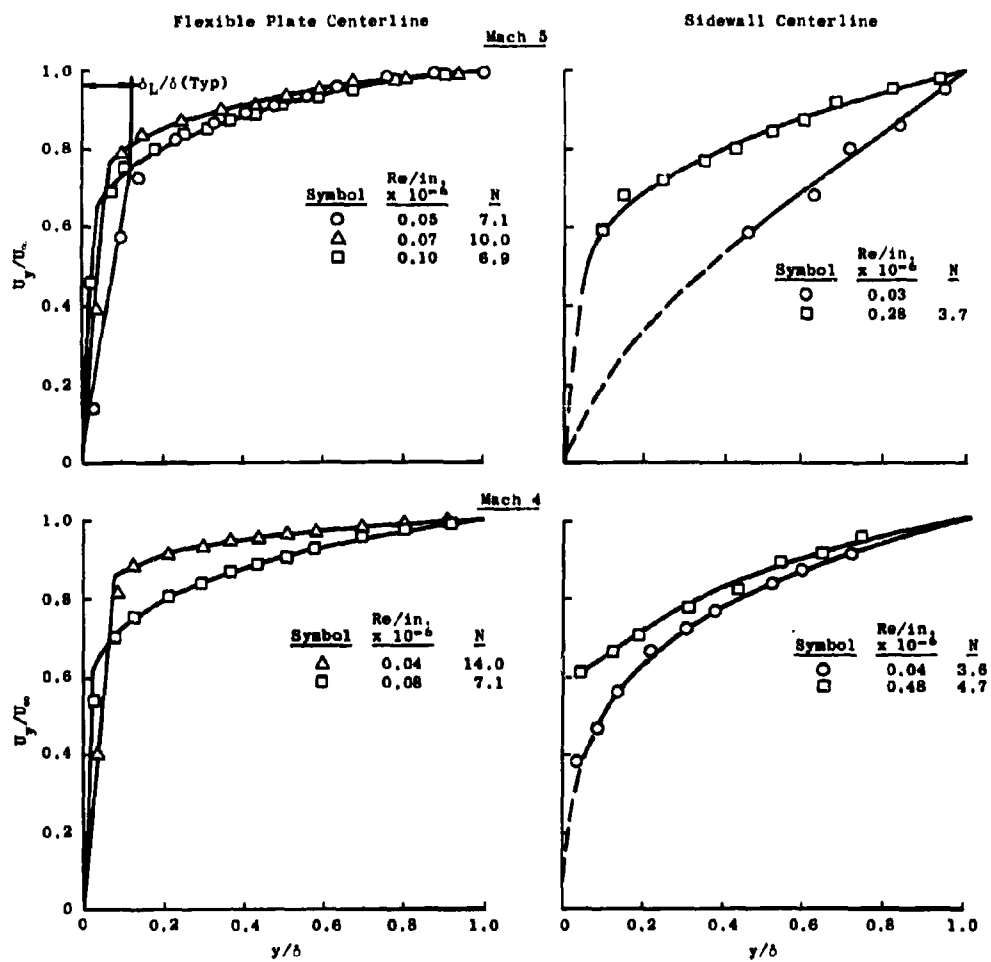


Fig. 4 Velocity Profiles on the Flexible Plate and Sidewall Centerlines at Mach Numbers 4 and 5

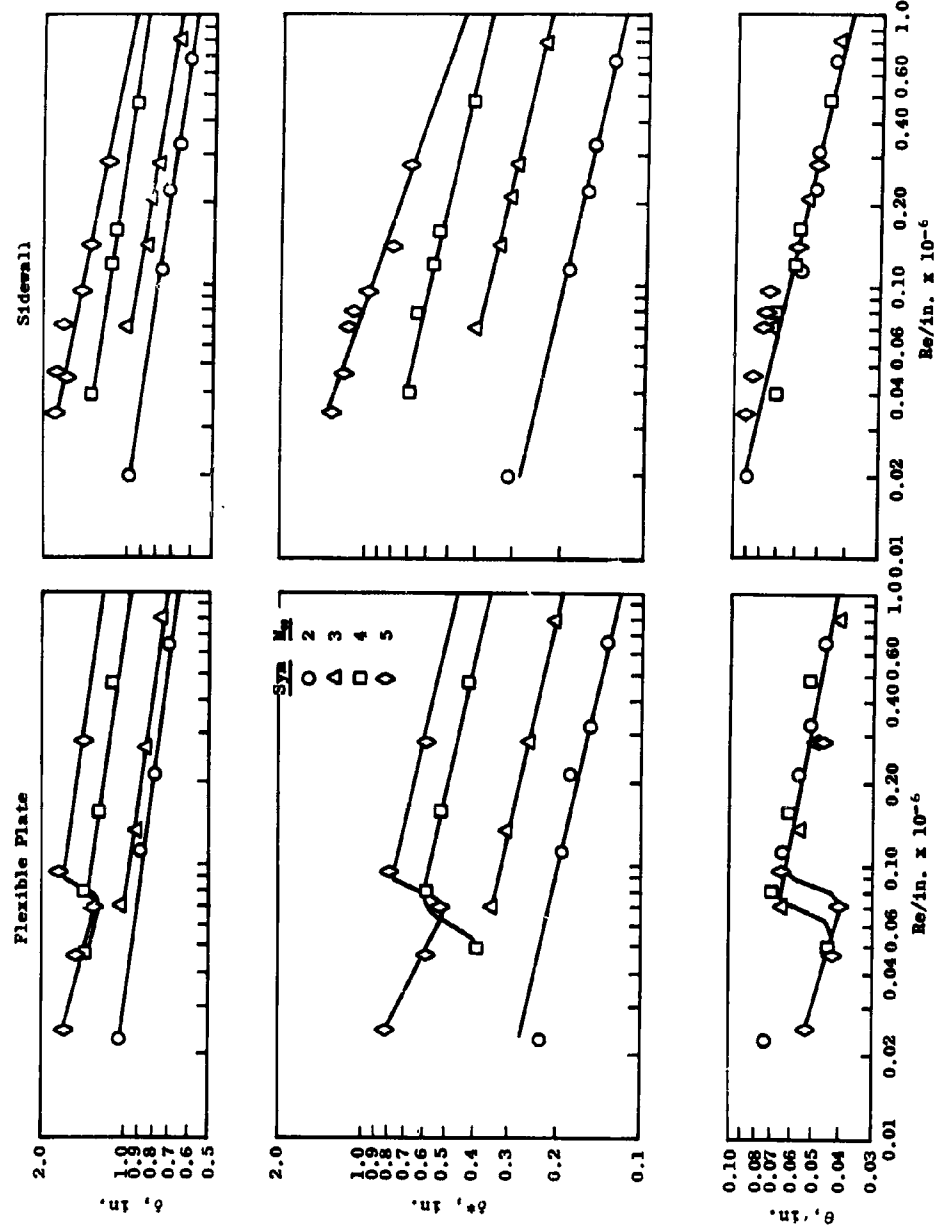


Fig. 5 Total, Displacement, and Momentum Thickness on the Flexible Plate and Sidewall Centerlines at Mach Numbers 2 through 5

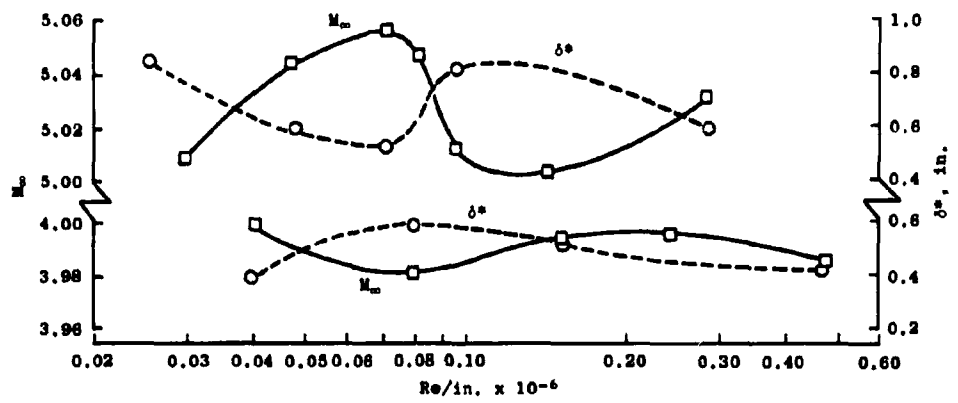


Fig. 6 Mach Number and Displacement Thickness Variation with Reynolds Number at Mach Numbers 4 and 5

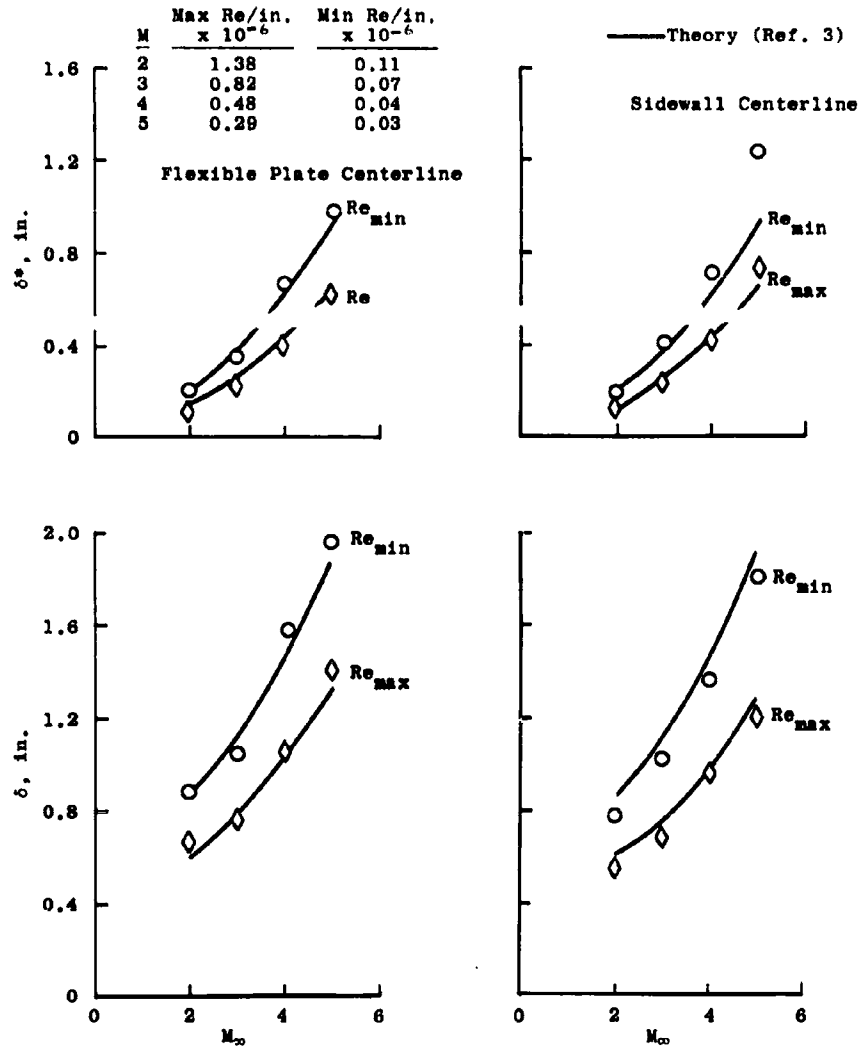


Fig. 7 Comparison between Experimental and Theoretical Values of Total and Displacement Thickness on the Flexible Plate and Sidewall Centerline at Mach Numbers 2 through 5

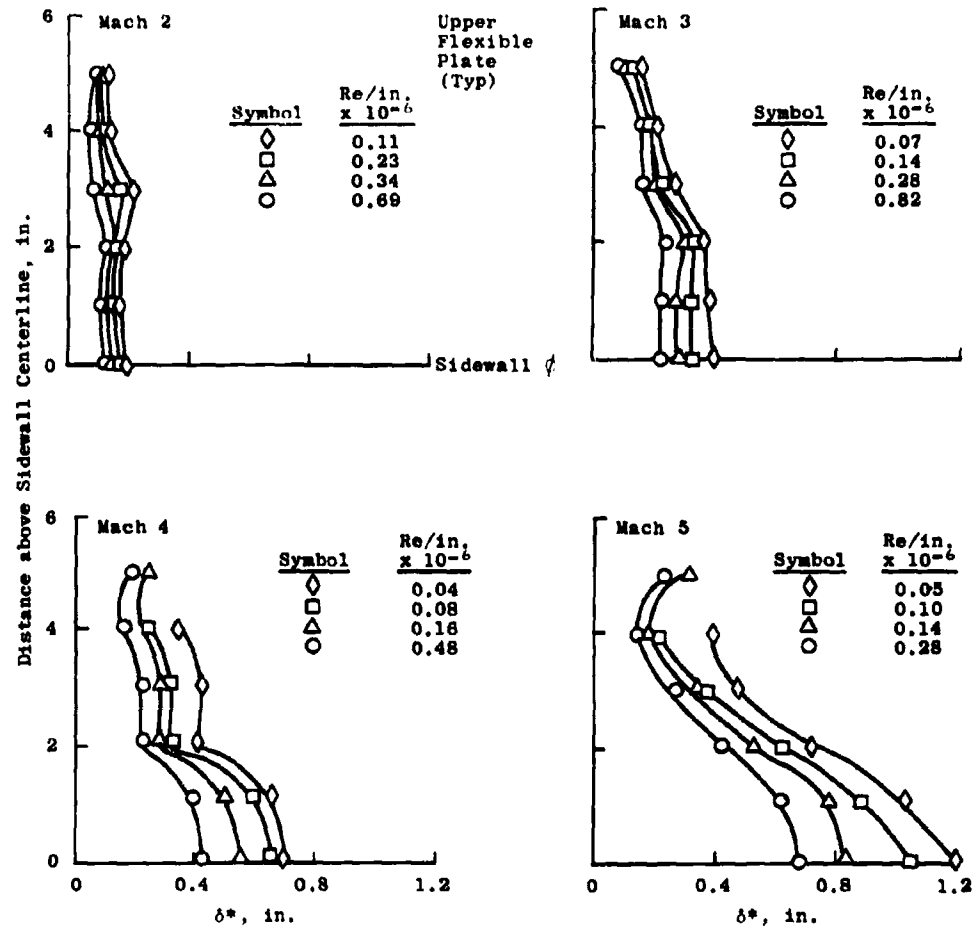


Fig. 8 Variation of the Sidewall Displacement Thickness between the Centerline and Upper Flexible Plate at Mach Numbers 2 through 5

Symbol	Facility	Test Section	Ref.
* ○	AEDC (VKF)	12" x 12"	
* □	AEDC (VKF)	40" x 40"	7
* △	AEDC (PWT)	12" x 12"	6
◇	JPL	20" x 20"	8
◇	JPL	20" x 20"	9
* ○	NASA	3.84" x 10"	5
○	OAL	19" x 27.5"	10
* ◇	DRL	1.45" x 1.45"	11
▽	RAE	8' x 8'	12
▽	UTIA	5" x 7"	13
* ○	NSL	18" x 24"	14

* δ^* computed at aerodynamic exit plane.

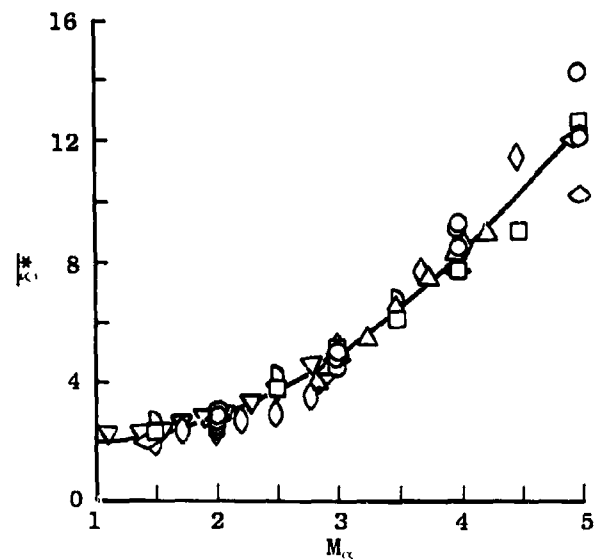


Fig. 9 Flexible Plate Displacement Thickness Correlation at Mach Numbers 1.5 through 5